

# INCREASING THE BEARING CAPACITY OF ROOF BOLTING WITH FRICTION-FASTENED ANCHOR BOLTS WHILE REDUCING ITS METAL CONSUMPTION THROUGH THE USE OF W-SECTION ANCHOR BOLTS

*Krechetov Andrey, T.F. Gorbachev Kuzbass State  
Technical University, PhD, Associate Professor*



## **Abstract**

A lot of contemporary research effort is aimed at increasing the efficiency of roof bolting with the use of friction-fastened anchor bolts. One of the solutions to this challenge is the use of W-section anchor bolts designed and patented by OKS LLC. The use of this type of anchor bolts makes it possible to increase the bearing capacity of roof bolting without using any additional materials and the need for additional operations. This paper assesses the maximum allowable loads, the stress-strain state and the expansion force during the installation of C-section friction anchor bolts with 3 mm thick walls, which are the most common at present, as well as W-section friction anchor bolts with 2 mm, 2.5 mm and 3 mm thick walls, respectively, into a borehole. In order to evaluate the efficiency of a particular section in terms of metal consumption, it was proposed to use the ratio of the generated expansion force to anchor bolt weight. For the C-section anchor bolts with 3 mm thick walls, this value is 57 kN/kg, while for the W-section anchor bolts with 2 mm, 2.5 mm and 3 mm wall thicknesses this value is 109 kN/kg, 114 kN/kg and 157 kN/kg, respectively.

## Introduction

At the present, roof bolting with the use of friction-fastened anchor bolts is widely used for rock reinforcement in mine workings [1-7]. This type of bolting has a number of advantages in comparison with other types of supports: relative simplicity of installation, increased efficiency of the rock reinforcement process, the possibility of loading the bolting immediately after its installation.

The friction anchor bolt is retained in the borehole through friction between the walls of the anchor bolt rod and the walls of the borehole. The ultimate bearing capacity of friction anchor bolts is evaluated by means of a pull-out test [8-9]. Research results show that friction anchor bolts have a relatively low bearing capacity, in most cases 40-60 kN per 1 meter of anchor bolt length [10]. After some time it can increase due to various phenomena: rock shear perpendicular to the borehole axis [11], corrosion of the anchor bolt rod [12] and others.

One of the key factors determining the bearing capacity of friction anchor bolts is the value of the anchor bolt expansion force on the borehole walls. A large number of technical solutions have been developed to increase this characteristic [10-19].

The operating principle of friction-fastened expansion anchor bolts is based on introducing a composite mixture into the anchor bolt rod after its installation; this mixture expands over time. When this mixture is introduced into the anchor bolt rod without inserting the anchor bolt into the borehole, the anchor bolt diameter increases by 11% after 4 days, and by 19% after 56 days [10]. Such a solution makes it possible to increase the anchor bolt's bearing capacity, but the full loading of the roof bolting of this type is only possible after a sufficiently long time has elapsed since installation. This leads to a reduction of fastening efficiency, thus rendering necessary the use of additional materials, which negatively affects the unit cost of fastening an anchor bolt.

Another way to increase the expansion force exerted by anchor bolts on the borehole walls is through the use of various versions of the friction anchor bolts with an expansion element, whereby the latter can be a solid rod, a hollow solid tube or a cut tube. The expansion element is either installed after the installation of the anchor bolt, or connected to the anchor bolt in a certain way and installed together with it [16 -19]. This solution allows to increase the expansion force of the anchor bolt, but the additional element increases the anchor bolt's metal consumption as well as the cost of its production and, consequently, the final cost to the consumer.

The purpose of this paper is to estimate the ultimate allowable loads, the stress-strain state and the expansion force generated by the ATF-type W-section anchor bolts of various wall thicknesses, designed and patented by OKS LLC [20], and to compare these characteristics to those of the C-section anchor bolt, the type most common to date.

## Methods

The ATF-type W-section friction-fastened tubular anchor bolt is a version of the friction-fastened anchor bolt which differs from the most common — C-section — anchor bolt type by the presence of inwardly bent edges in the area of the anchor bolt's longitudinal slot. When this type of anchor bolt is installed into a borehole and its outer diameter is reduced, the bent edges of the longitudinal slot come into contact, and the section stiffness increases significantly; as a result, the expansion force is increased. A significant advantage of the ATF-type W-section anchor bolt is that no additional materials or operations are required for its installation.

In this paper, the expansion force of the C-section anchor bolts with 3 mm thick walls (hereinafter C3) and W-section anchor bolts with wall thicknesses of 2 mm, 2.5 mm and 3 mm (hereinafter W2, W2.5 and W3, respectively)

were evaluated. The C-section is shown in Fig. 1a, the W-section with 3mm thick walls is shown in Fig. 1b. The characteristics of the sections and of the corresponding anchor bolts are given in Table 1.

Table 1

Characteristics of anchor bolt sections with various wall thicknesses

Section	S, mm <sup>2</sup>	m, kg	I <sub>xx</sub> , mm <sup>4</sup>	ΔS, %	Δm, %	I <sub>xx</sub> , %
C3	346.8	2.71	64,727.2			
W2	291.6	2.27	59,592.9	-15.93	-15.93	-7.93
W2.5	350.7	2.74	70,371.6	+1.11	+1.11	+8.72
W3	424.2	3.31	82,683.9	+22.30	+22.30	+27.74

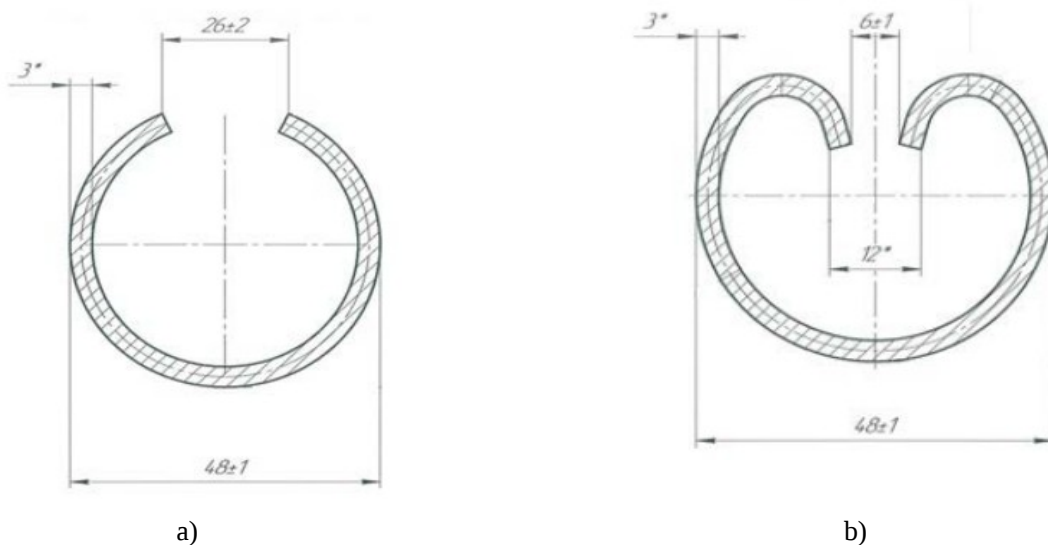


Figure 1. Friction-fastened anchor bolt section: a) ATF-type C-section with 3 mm thick walls; b) ATP-type W-section with 3 mm thick walls

Designations in Table 1 are:  $S$  - cross-sectional area;  $m$  - weight of 1 m of the anchor bolt;  $I_{xx}$  - moment of inertia of the section relative to the  $x$  axis (i.e. the horizontal axis, see Fig. 1);  $\Delta S$  - change in the section area as compared to section C3;  $\Delta m$  - change in weight of 1 m of anchor bolt as compared to that of the section C3 anchor bolt, and  $\Delta I_{xx}$  - change in moment of inertia of the section as compared to section C3.

From the analysis of the Table 1 data, it can be seen that the W2-section anchor bolt has a weight 16% less than the C3-section anchor bolt, but due to the geometry of the section the moment of inertia  $I_{xx}$  is reduced by a lower value of 8 %. The W2.5-section anchor bolt has a weight comparable to the C3-section anchor bolt, whereby the moment of inertia  $I_{xx}$  increases by 9%. The W3-section anchor bolt has a greater weight than the C3-section anchor bolt, but also a 28% higher moment of inertia  $I_{xx}$ .

The maximum allowable load on the anchor bolt rod in the case of its application along the longitudinal axis was determined by its yield strength  $\sigma_{0.2}$  and ultimate tensile strength  $\sigma_b$ :

$$P_{0.2} = S\sigma_{0.2}, \quad (1)$$

$$P_b = S\sigma_{ob}. \quad (2)$$

As the values of the ultimate stresses, the minimum values of  $\sigma_{0.2}$  and  $\sigma_b$  for rolled steel up to 10 mm thick, St3ps grade, GOST 535-2005, were assumed, taking into account the requirements of GOST 31559-2012 for roof bolting with the use of friction-fastened anchor bolts. The assumed values are 245 MPa and 410 MPa, respectively.

$M_x^{max}$ , the maximum allowable bending moment with respect to the  $x$  axis was estimated using the finite element method. For this purpose, the anchor bolt rod was simulated with rod elements. The point of the anchor rod axis at the beginning of the coordinate system was rigidly fixed, a force  $P_{Mx}$  was applied to the opposite end of the anchor bolt rod axis (Fig. 2 a). The material properties corresponded to those of the St3ps steel grade. During the simulation, the maximum force value  $P_{Mx}$  was determined at which the arising stresses did not exceed the yield strength  $\sigma_{0.2}$  (Fig. 2 b). This value was then multiplied by the length of the anchor bolt rod to estimate the maximum allowable moment.

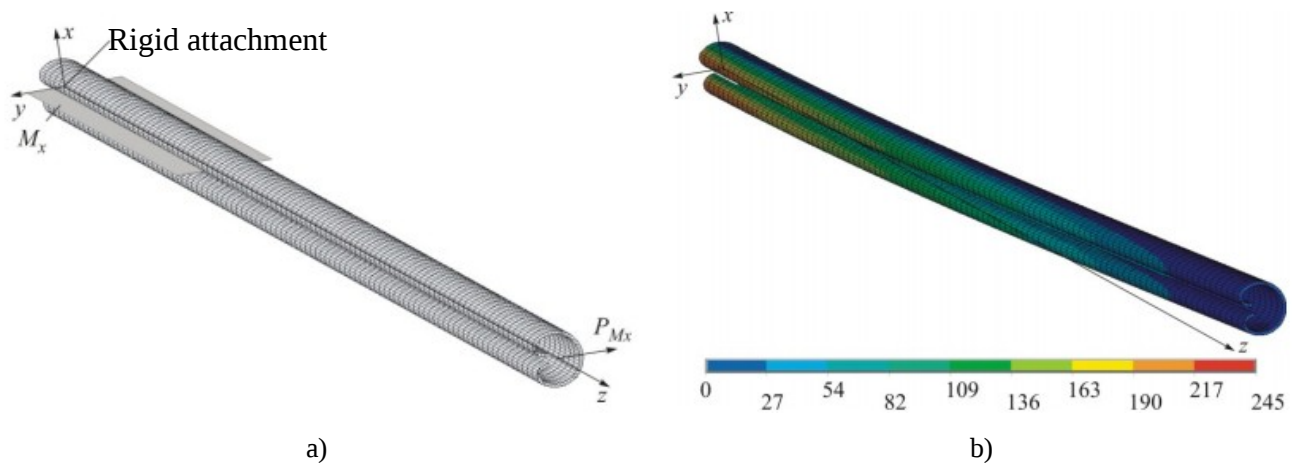


Figure 2. Simulation of anchor bolt rod bending: a) - finite element method; b) - stress intensity at the maximum allowable force  $P_{Mx}$  (MPa)

The expansion force generated by 48 mm anchor bolts with various section types, when installed into a 43 mm diameter borehole, was also determined using the finite element method. For this purpose, a finite element model was created consisting of a unit length (1 mm) section of the anchor bolt and an elastic ring on the outside of the anchor bolt section (Fig. 3). The material properties of the anchor bolt section corresponded to the St3ps steel grade, and the plastic properties were also determined for this material by setting the corresponding flow curve.

Contact interaction was simulated between the outer side of the anchor bolt section and the inner side of the elastic ring; to optimize the calculation procedure, the condition for contact interaction was to maintain contact when the model was loaded. The contact interaction was also simulated between surfaces of the longitudinal slot edges in an ATP-type W-section anchor bolt; those surfaces were in contact with each other during the installation of the anchor bolt into a borehole.

The end surfaces of the anchor bolt section and the elastic ring were subjected to a displacement constraint relative to the  $z$  axis. Thus, the stress-strain state was calculated for the case of a plane-strain deformation. Displacements were applied to the outer side of the elastic ring so that the inner side of the elastic ring took the form of a borehole - a circle with a 43 mm diameter (Fig. 4).

As a result of the simulation, the values of stresses and deformations were determined. The value of the expansion force was estimated as the reaction force of the support in the contact pair between the anchor bolt section and the elastic ring in the cylindrical coordinate system directed radially (in the direction of the  $x$  axis when rotated  $360^\circ$ , see Fig. 5).

Elastic ring: diameter shrinks down to 43 mm

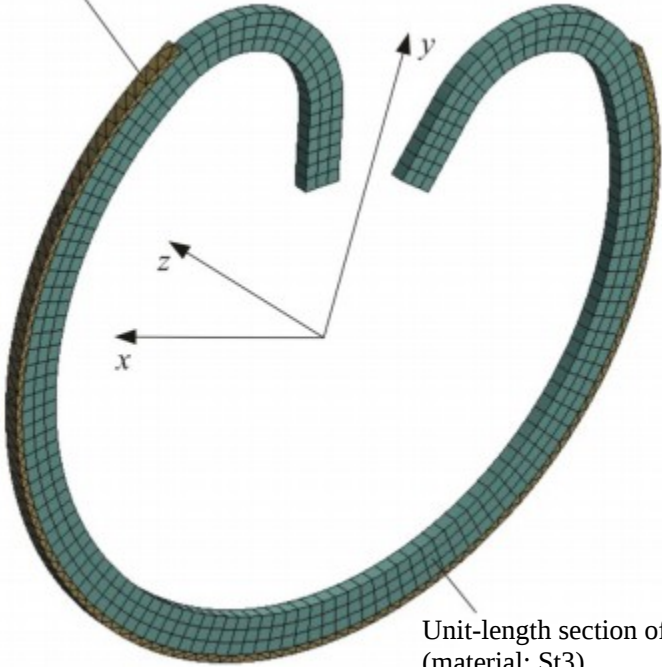


Figure 3. Finite element model of the anchor bolt and elastic ring cross section

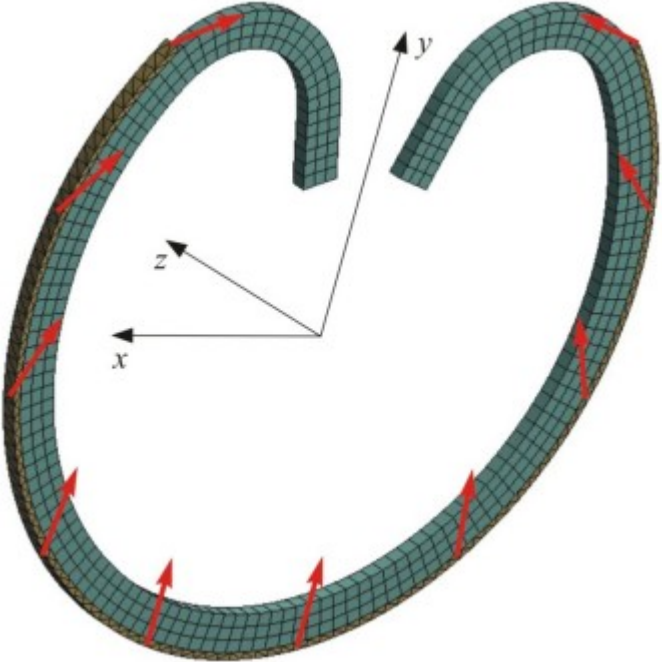


Figure 4. Displacements applied to the elastic ring

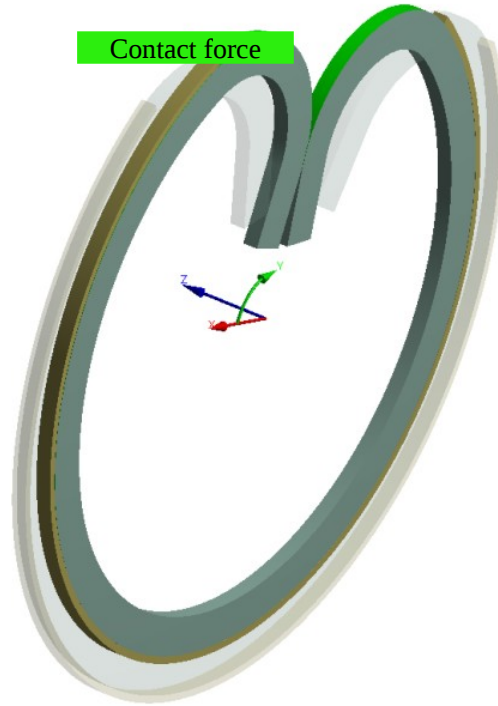


Figure 5. Estimating the expansion force during the anchor bolt installation into a borehole

## Results and Discussion

The maximum allowable loads on the anchor bolt rod are given in Table 2.

Table 2

Maximum allowable loads on the anchor bolt rod

Section	$P_{0.2}$ , kN	$P_B$ , kN	$M_x^{max}$ , N·m	$\Delta P_{0.2}$ , %	$\Delta P_B$ , %	$\Delta M_x^{max}$ , %
C3	84.98	128.33	630.18			
W2	71.44	107.89	634.32	-15.93	-15.93	+0.66
W2.5	85.92	129.76	760.68	+1.11	+1.11	+20.71
W3	103.93	156.95	884.52	+22.3	+22.3	+40.36

Designations in Table 2 are:  $P_{0.2}$  - maximum allowable force at the yield strength;  $P_B$  - maximum allowable force at the ultimate tensile strength;  $M_x^{max}$  - maximum allowable bending moment relative to  $x$  axis;  $\Delta P_{0.2}$  - change in maximum force at the yield strength as compared to the C3-section anchor bolt;  $\Delta P_B$  - change in maximum force at the ultimate tensile strength as compared to the C3-section anchor bolt;  $\Delta M_x^{max}$  - change in maximum allowable moment relative to  $x$  axis as compared to the C3-section anchor bolt.

The analysis of the results in Table 2 shows that the maximum allowable loads on the W2-section anchor bolt rod are 16% less than those on the C3-section anchor bolt rod, while the allowable bending moment for this type of section has a greater value. The allowable loads on the W2.5-section anchor bolt rod are comparable to those on the

C3-section anchor bolt rods, while the allowable bending moment is 20% higher. The allowable loads on the W3-section anchor bolts are 22% higher than those on the C3-section anchor bolts, the allowable bending moment is 40 % higher.

Despite the lower values of the allowable load on the W2-section anchor bolt rod in comparison with the C3-section anchor bolt rod, the minimum value (71.44 kN at the yield strength) is by 43% greater than the normative minimum allowable load (50 kN according to GOST 31559-2012). Also important is the fact that the friction anchor bolt transfers part of the load to the borehole walls due to the expansion force. Therefore, when the friction anchor bolt is loaded until it shifts in the borehole, the bearing capacity is determined not only by the anchor bolt rod, but also by the surrounding rock. This is the reason why, in some cases, the pulling force during the pull-out test is greater than the allowable load, not only at the yield strength, but even at the ultimate tensile strength. In this regard, the expansion force generated by the anchor bolt when it is installed into a borehole is decisive for increasing the bearing capacity.

The expansion force for the sections is given in Table 3. The table shows the values of the expansion force for the unit-length obtained as a result of the simulation, for the anchor bolt rod length of 1850 mm and 2700 mm. The change in the expansion force compared to C3-section anchor bolts is also shown, designated  $\Delta F_p$ .

Fig. 6 demonstrates the stress intensity distribution when anchor bolts with different sections are installed into a borehole; Fig. 7 shows the distribution of plastic strain intensity.

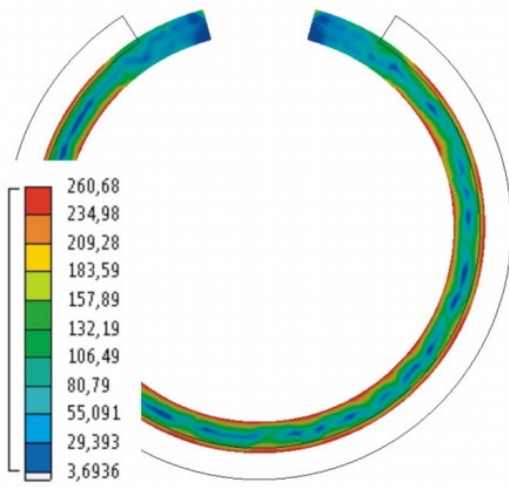
The analysis of the stress intensity distribution shows that the stress for section C3 has a minimum value for all simulated sections and amounts to 260 MPa. The intensity of stresses is the highest for section W2.5 and reaches 311 MPa; for section W3 it decreases to 301 MPa. The intensity of plastic strains in the W-sections is concentrated in the areas where the bent edges of the section originate, and it increases along with the thickness from 0.016 for section W2 to 0.036 for section W3.

The expansion force of W-section anchor bolts is much higher than that of C-section anchor bolts. For example, the expansion force of a W2 anchor bolt, which weighs 16 % less than a C3 anchor bolt, is 60% higher. The expansion force of the W2.5-section anchor bolt is more than twice as high as that of the C3-section anchor bolt, although the relative weight of the two is comparable. The W3-section anchor bolt provides more than 3 times the expansion force of the C3-section anchor bolt, whereby the anchor has a 22% increase in weight. The increase in the expansion force of the W-section anchor bolts is achieved by the contact interaction of the bent edges, and the edges coming together have the effect of increasing the section's stiffness considerably.

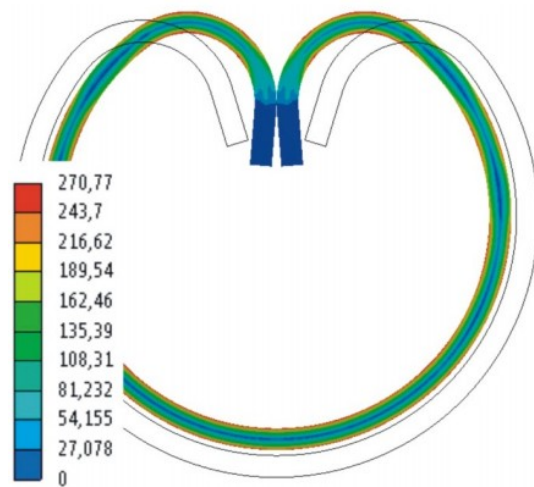
Table 3

Expansion force values

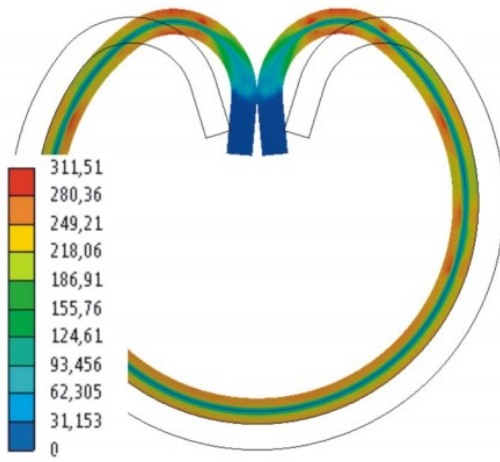
Section	Expansion force $F_p$ , kN			
	per 1 mm of length	per 1,850 mm of length	per 2,700 mm of length	$\Delta F_p$ , %
C3	0.155	286.75	418.5	
W2	0.248	458.8	669.6	+60
W2.5	0.312	577.2	842.4	+101
W3	0.521	963.85	1,406.7	+236



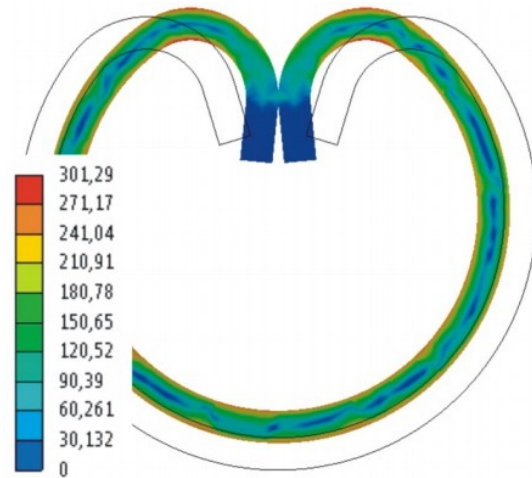
a)



b)



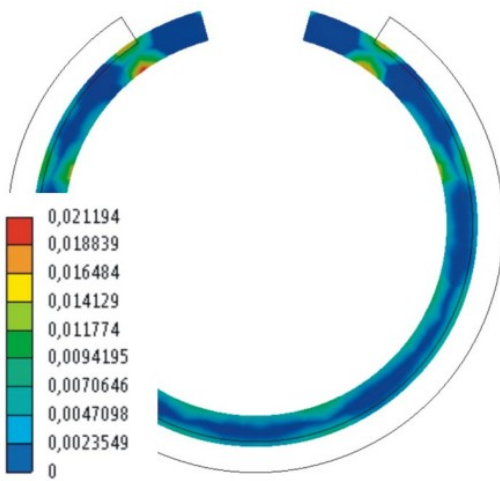
c)



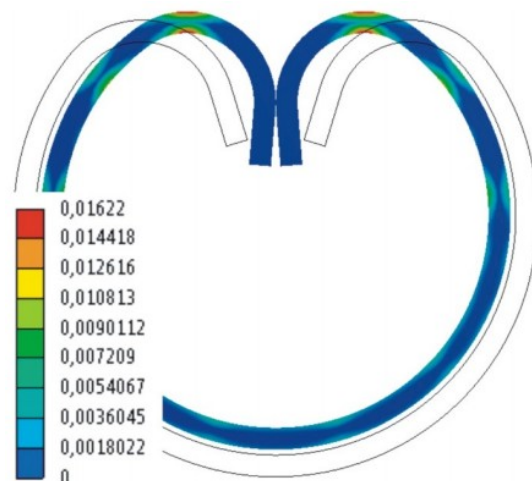
d)

Figure 6. Stress intensity distribution during the anchor bolt installation into a borehole, MPa:

a) C3 section; b) W2 section; c) W2.5 section; d) W3 section



a)



b)



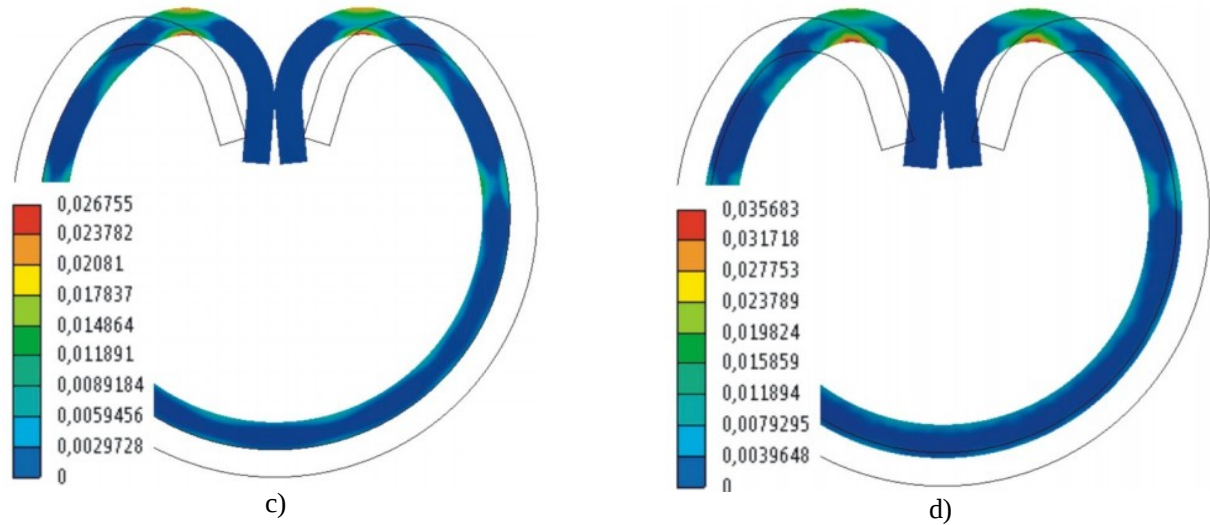


Figure 7: Distribution of plastic strain intensity during the installation of an anchor bolt into a borehole, MPa:  
a) C3 section; b) W2 section; c) W2.5 section; d) W3 section

The efficiency of a section in terms of metal consumption can be evaluated using the ratio of the expansion force to the anchor bolt weight:

$$\frac{F_{p1M}}{m_{1M}}, \quad (3)$$

where  $F_{p1M}$  is the expansion force for an anchor bolt length of 1 m;  $m_{1M}$  is the weight of 1 m of the anchor bolt.

For the C-section anchor bolts with 3 mm thick walls this value is 57 kN/kg, for the W-section anchor bolts with wall thicknesses of 2 mm, 2.5 mm and 3 mm, respectively, it is 109 kN/kg, 114 kN/kg and 157 kN/kg. Thus, the W-section friction-fastened anchor bolts are much more efficient in terms of metal consumption.

The expansion force values obtained can be used to predict the bearing capacity of the anchor bolts. The shear resistance of the anchor bolt corresponds to the friction force between the walls of the anchor bolt rod and the borehole walls, and can be calculated using the formula:

$$F_{c\bar{d}}^* = F_{\tau p} = \mu F_p, \quad (4)$$

where  $\mu$  is the coefficient of friction between the walls of the anchor bolt rod and the borehole walls.

According to the reference data, the friction coefficient of steel on rock is between 0.25 and 0.5 depending on the conditions. Accordingly, the shear force  $F_{c\bar{d}}$  for a W2-section anchor bolt with a rod length of 1850 mm can reach up to 229.4 kN, and for a W2.5-section anchor bolt it can reach up to 288.6 kN. As noted above, the anchor bolt and the surrounding rock work together until the anchor bolt shifts in the borehole due to the expansion force during loading; therefore, the bearing capacity of a friction-fastened anchor bolt is determined by the shear force. The obtained design values are confirmed by the results of pilot tests - during pull-off tests, the limit load of W3-section anchor bolts was 260 kN in some cases.

It should be taken into account that the real value of the shear force may be less than the calculated one due to a damage to the integrity of the borehole walls, as well as increased rock fracturing in the borehole drilling zone.

However, all other things being equal, a W2-section anchor bolt will have a 60% higher bearing capacity than a C3-section anchor bolt; a W2.5-section anchor bolt will have twice the bearing capacity of a C3-section anchor bolt, and a W3-section anchor bolt will have 3.6 times the bearing capacity of a C3-section anchor bolt.

\* Hereinafter  $F_{c\bar{d}}$  stands for shear force,  $F_{\tau p}$  for friction force.

## Conclusion

1. In the present paper, we have evaluated the ultimate allowable loads, the stress-strain state and the expansion force during the installation of the ATF-type C-section tubular friction anchor bolts with 3mm thick walls and the ATF-type W-section friction anchor bolts with wall thicknesses of 2 mm, 2.5 mm and 3 mm, in a borehole.
2. It has been found that the ultimate allowable loads for the ATF-type W-section anchor bolt rod are greater than those for the ATF-type C-section anchor bolt rod. The exception is the ATF-type W-section anchor bolt with 2 mm thick walls, however the minimum limit value (71.44 kN at the yield strength) is by 43 % higher than the minimum allowable normative values (50 kN according to GOST 31559-2012). In addition, the weight of this version of the anchor bolt is 16 % less than that of the ATF-type C-section anchor bolt with 3 mm thick walls, while the maximum allowable bending moment of this version is higher.
3. It has been shown that W-section anchor bolts provide a higher value of the expansion force compared to the C-section anchor bolts by a factor of 1.6, 2 and 3.6 for the W-section anchor bolts with wall thicknesses of 2 mm, 2.5 mm and 3 mm, respectively.
4. W-section is more efficient in terms of metal consumption. For the C-section anchor bolts with 3 mm thick walls, the ratio of the expansion force to the anchor bolt weight is 57 kN/kg, while for the W-section anchor bolts with wall thicknesses of 2 mm, 2.5 mm and 3 mm this value is 109 kN/kg, 114 kN/kg and 157 kN/kg, respectively.
5. It has been found that the shear force of an anchor bolt relative to borehole walls can reach the value of 229.4 kN in case of a W-section anchor bolt with 2 mm thick walls and a 1850 mm long rod, and can reach 288.6 kN in case of a similar anchor bolt with 2.5 mm thick walls; the calculated results correlate well with the results of pilot tests.
6. It has been demonstrated that since the bearing capacity of a friction anchor bolt is determined by the friction force of the anchor bolt walls and the borehole walls and since the friction force is directly proportional to the expansion force, other things being equal, the bearing capacity of the W-section anchor bolts with wall thicknesses of 2 mm, 2.5 mm and 3 mm are, respectively, 1.6, 2 and 3.6 times higher than that of the C-section anchor bolts.
7. For normal operating conditions, it is recommended to use W-section anchor bolts with 12 mm thick walls, which, in comparison with C-section anchor bolts, provide a 1.6 times increase in bearing capacity while reducing the anchor bolt's metal consumption by 16%.
8. For difficult operating conditions, it is recommended to use W-section anchor bolts with 2.5 mm thick walls, which, in comparison with C-section anchor bolts, provide a 2-fold increase in the bearing capacity, although both types of anchor bolts are comparable in terms of metal consumption.
9. For particularly difficult operating conditions, it is recommended to use W-section anchor bolts with 3 mm thick walls, which, in comparison with C-section anchor bolts, provide a 3.6 times increase in the bearing capacity while slightly increasing the anchor bolt's metal consumption (by 22%).

## References

10. Zubkov A.A., Latkin V.V., Neugomonov S.S., Volkov P.V. Prospective methods of supporting mine workings at underground mines // Mining Informational and Analytical Bulletin (Scientific and Technical Journal). - 2014. no. S1-1 p. 106-117.
11. Rahimi B., Sharifzadeh M., Feng X. Ground behavior analysis, support system design and construction strategies in deep hard rock mining – Justified in Western Australian's mines // Journal of Rock Mechanics

- and Geotechnical Engineering. Volume 12, Issue 1, February 2020, Pages 1-20. <https://doi.org/10.1016/j.jrmge.2019.01.006>.
12. Ghorbani M., Shahriar K., Sharifzadeh M., Masoudi R. A critical review on the developments of rock support systems in high stress ground conditions // International Journal of Mining Science and Technology. Volume 30, Issue 5, September 2020, Pages 555-572. <https://doi.org/10.1016/j.ijmst.2020.06.002>.
  13. Li C.C. Principles and methods of rock support for rockburst control // Journal of Rock Mechanics and Geotechnical Engineering. Volume 13, Issue 1, February 2021, Pages 46-59. <https://doi.org/10.1016/j.jrmge.2020.11.001>.
  14. Toscano-Alor C., Castillo-Rodil A., Pehovaz-Alvarez H., Raymundo C., Mamani-Macedo N., Moguerza J.M. (2020) Hydrabolt and Split Set Rock Bolt Selection Method Under the Bieniawski Rock Mass Rating for Improving Horizontal Access Support in Peruvian Mid-Scale Mining Activities. In: Kantola J., Nazir S., Salminen V. (eds) Advances in Human Factors, Business Management and Leadership. AHFE 2020. Advances in Intelligent Systems and Computing, vol 1209. Springer, Cham. [https://doi.org/10.1007/978-3-030-50791-6\\_46](https://doi.org/10.1007/978-3-030-50791-6_46).
  15. Li C.C. Principles of rockbolting design // Journal of Rock Mechanics and Geotechnical Engineering. Volume 9, Issue 3, June 2017, Pages 396-414. <https://doi.org/10.1016/j.jrmge.2017.04.002>.
  16. Li C.C. Rockbolting. Principles and Applications. Butterworth-Heinemann. 2018. 284 p. ISBN: 978-0-12-804401-8. <https://doi.org/10.1016/C2015-0-01742-7>.
  17. Tomory, P.B., Grabinsky, M., Curran, J., & Carvalho, J. (1998). Factors influencing the effectiveness of Split Set friction stabilizer bolts. Cim Bulletin, 91, 205-214.
  18. Nicholson L., Hadjigeorgiou J.(2018) Interpreting the results of in situ pull tests on Friction Rock Stabilizers (FRS), Mining Technology, 127:1, 12-25, <https://doi.org/10.1080/14749009.2017.1296669>.
  19. Davison G.R., Fuller P.G. 2013. Investigation of expanding Split Sets. In: Potvin Y., Brady B. (eds), Proceedings of the Seventh International Symposium on Ground Support in Mining and Underground Construction, Australian Centre for Geomechanics, Perth, pp. 163-170, [https://doi.org/10.36487/ACG\\_rep1304\\_09\\_Davison](https://doi.org/10.36487/ACG_rep1304_09_Davison)
  20. Zubkov A. A., Kalmykov V. N., Kutlubaev I. M., Naidenova M. S. Justification of the characteristics of roof boltings with the use of friction-fastened anchor bolts // Mining Information Analytical Bulletin. - 2019. - No 10. - C. 35-43. <https://doi.org/10.25018/0236-1493-2019-10-0-35-43>.
  21. Stimpson B. Split Set friction stabilizers: an experimental study of strength distribution and the effect of corrosion. Canadian Geotechnical Journal. 35(4): 678-683. <https://doi.org/10.1139/t98-025>.
  22. Xu S., Yang Z., Caiab M. Hou P. An experimental study on the anchoring characteristics of an innovative self- swelling Split-set // Tunnelling and Underground Space Technology. Volume 112, June 2021. <https://doi.org/10.1016/j.tust.2021.103919>.
  23. Hao Y., Wua Y., Ranjith P.G., Zhang K., Hao G., Teng Y. A novel energy-absorbing rock bolt with high constant working resistance and long elongation: Principle and static pull-out test // Construction and Building Materials. Volume 243, 20 May 2020. <https://doi.org/10.1016/j.conbuildmat.2020.118231>.
  24. Cai M., D. Champaigne, Coulombe J.G., Challagulla K. Development of two new rockbolts for safe and rapid tunneling in burst-prone ground // Tunnelling and Underground Space Technology. Volume 91, September 2019. <https://doi.org/10.1016/j.tust.2019.103010>.

25. Kopytov A.I., Voytov M.D., Tripus T.E. Calculation of the friction-type tubular anchor bolt for bearing capacity // Bulletin of Kuzbass State Technical University. 2012. № 4 (92). C. 8- 10.
26. Masaev Yu.A., Politov A.P., Kopytov A.I., Masaev V.Y. Improved design of roof boltings for the erection of mine workings // Bulletin of Scientific Centre VostNII. - 4-2018. - p. 66-73.  
<https://doi.org/10.25558/VOSTNII.2018.8.24.006>.
27. Pershin V.V., Fadeev Yu.A., Tripus T.E. Justification of parameters and development of a new design of a multilayered friction-type anchor bolt // Proceedings of Higher Educational Institutions. Mining Journal. 2016. № 2. p. 47-53.
28. Zubkov A.A., Zubkov A.E., Zhdanova Yu.I. Reinforced self-locking roof bolting. Utility model patent RU 168801 U1, 21.02.2017. Application No. 2016134870 dated 25.08.2016.
29. Oks-Trade LLC: New generation friction-type anchor bolt // Mining Industry. 2017. № 6 (136). p. 54-55